Direct Numerical Simulations of Droplet Bag Breakup

ARCHER2 Celebration of Science 2025, The University of Edinburgh

Kaitao Tang[1], Thomas Adcock[1] and Wouter Mostert[1]

15/05/2025

[1] Environmental Fluid Mechanics Group,
Department of Engineering Science,
University of Oxford, Oxford, OX1 3PJ, UK

Introduction: Ocean Sprays

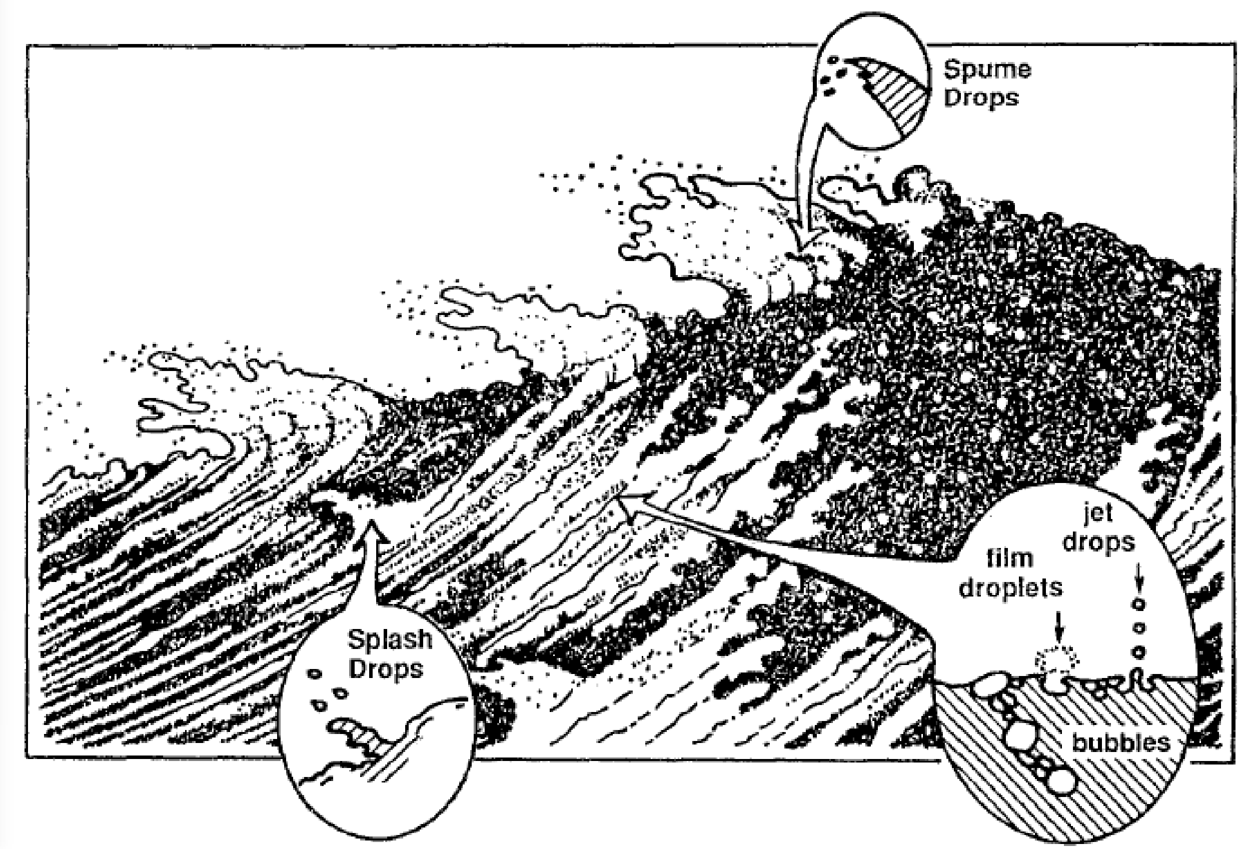

Major pathways of ocean spray generation

- Significance of Ocean Sprays
  - Enhancing air-sea mass, momentum and energy transfer
  - Small sprays: cloud nucleation sites
  - Large sprays: surface drag reduction for tropical cyclone formation
- Modulated by wave breaking
- Pathways of ocean spray generation
  - Bursting of entrained bubbles
  - **Spume drop ejection** under high winds
  - **Wave splashing** between different parts of breaking waves

[1] Andreas, E. L. *et al.* (1995). The spray contribution to net evaporation from the sea: A review of recent progress. *Boundary-Layer Meteorology*, *72*, 3-52.
[2] Veron, F. (2015). Ocean spray. *Annual Review of Fluid Mechanics*, *47*, 507-538.
[3] Deike, L. (2022). Mass transfer at the ocean–atmosphere interface: The role of wave breaking, droplets, and bubbles. *Annual Review of Fluid Mechanics*, 54, 191-224.

Introduction: Bag Breakup Phenomena

- Experiments by Troitskaya et al. [1]
  - Bags formed from small-scale sea surface perturbations
  - Dominates high-wind spume generation
  - Fragment size range: **100 – 1000 μm**
- Resembles low-We droplet [2] and thin film [3] breakup
  - Challenge in addressing multiscale physics

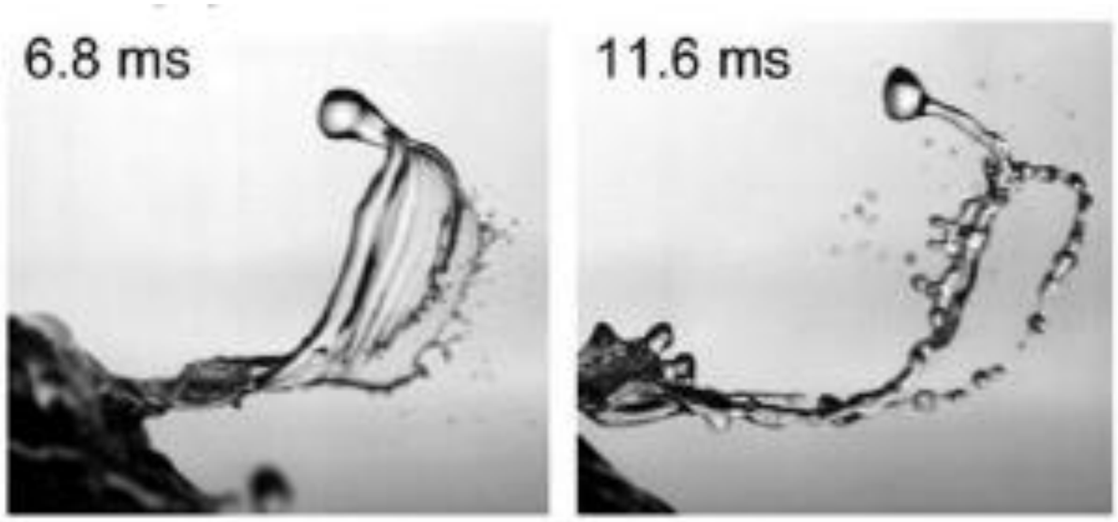

Breakup of small-scale air-sea interfacial disturbances [1].

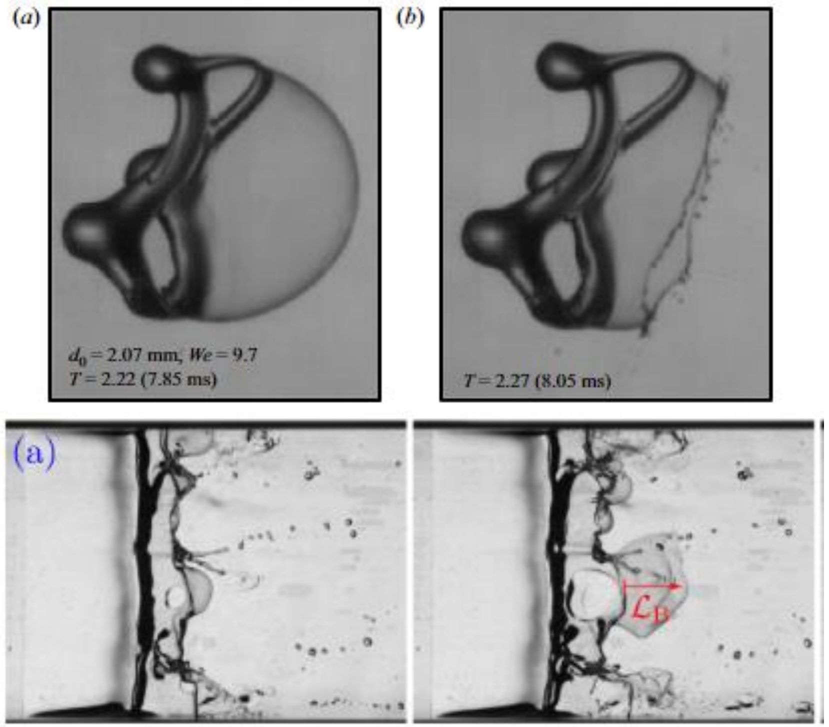

A droplet (upper row) [2] and a wind-sheared liquid film [3] undergoing bag breakup.

[1] Troitskaya, Y. et al. (2017). Bag-breakup fragmentation as the dominant mechanism of sea-spray production in high winds. *Scientific Reports*, 7(1), 1-4.
[2] Jackiw, I. M., & Ashgriz, N. (2022). Prediction of the droplet size distribution in aerodynamic droplet breakup. *Journal of Fluid Mechanics*, 940.
[3] Kant, P., Pairetti, C., Saade, Y., Popinet, S., Zaleski, S., & Lohse, D. (2023). Bag-mediated film atomization in a cough machine. *Physical Review Fluids*, 8(7), 074802.

Droplet Aerobreakup

- Breakup Regimes (for increasing We and $Oh \leq 0.1$):

  Vibrational
  Bag ($11 \leq We \leq 18$)
  Bag-stamen/multimode
  Sheet-thinning
  Catastrophic breakup

Gentle → Violent

$$We \equiv \frac{\rho_g U_0^2 d_0}{\sigma}, \qquad Oh \equiv \frac{\mu_l}{\sqrt{\rho_l \sigma d_0}}$$

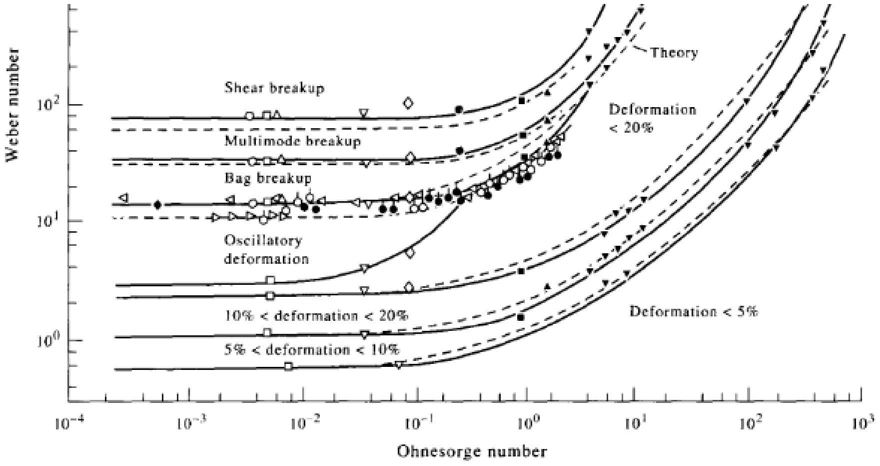

$We - Oh$ phase diagram for droplet breakup regimes [1].

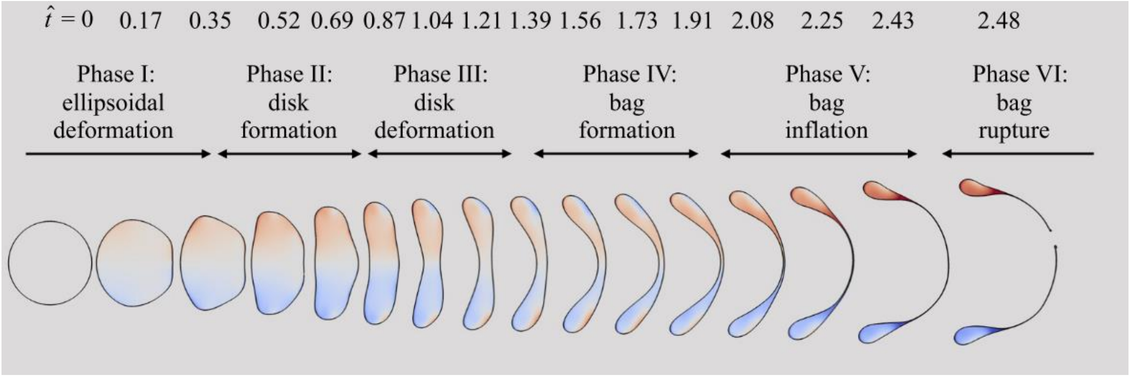

Droplet morphology recorded at $We = 12$ [3].

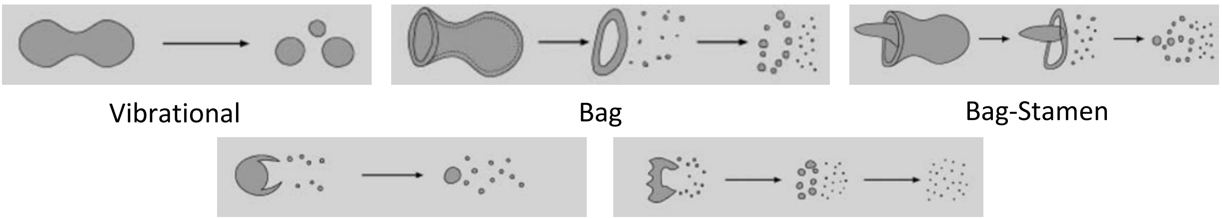

Droplet morphology in different breakup regimes as We increases [2].

[1] Hsiang, L. P., & Faeth, G. M. (1995). Drop deformation and breakup due to shock wave and steady disturbances. *International Journal of Multiphase Flow*, 21(4), 545-560.
[2] Guildenbecher, D. R., López-Rivera, C., & Sojka, P. E. (2009). Secondary atomization. *Experiments in Fluids*, 46(3), 371-402.
[3] Ling, Y., & Mahmood, T. (2023). Detailed numerical investigation of the drop aerobreakup in the bag breakup regime. *Journal of Fluid Mechanics*, 972, A28.

Laminar Bag Breakup

Tang, K., Adcock, T. A. A., & Mostert, W. (2023). *Bag film breakup of droplets in uniform airflows*. Journal of Fluid Mechanics, 970, A9. Featured on Cover.

Turbulent Bag Formation

Tang, K., Adcock, T. A. A., & Mostert, W. (2025). Droplet bag formation in turbulent airflows. Physical Review Fluids, 10(3), 033604. Selected as Editor's Suggestion

Formulation and Methodology: Numerical Setup

- The Basilisk Solver [1]
  - Two-phase, incompressible Navier-Stokes Equation w. surface tension
  - Finite-volume w. adaptive mesh refinement (AMR)
  - Geometric volume-of-fluid (VOF) interface reconstruction
- Simulation configurations
  - Fully 3D simulations
    - Necessary for **post-breakup** fragment statistics
    - High computational cost
  - Axisymmetric simulations
    - **Pre-breakup drop deformation**
    - Low computational cost

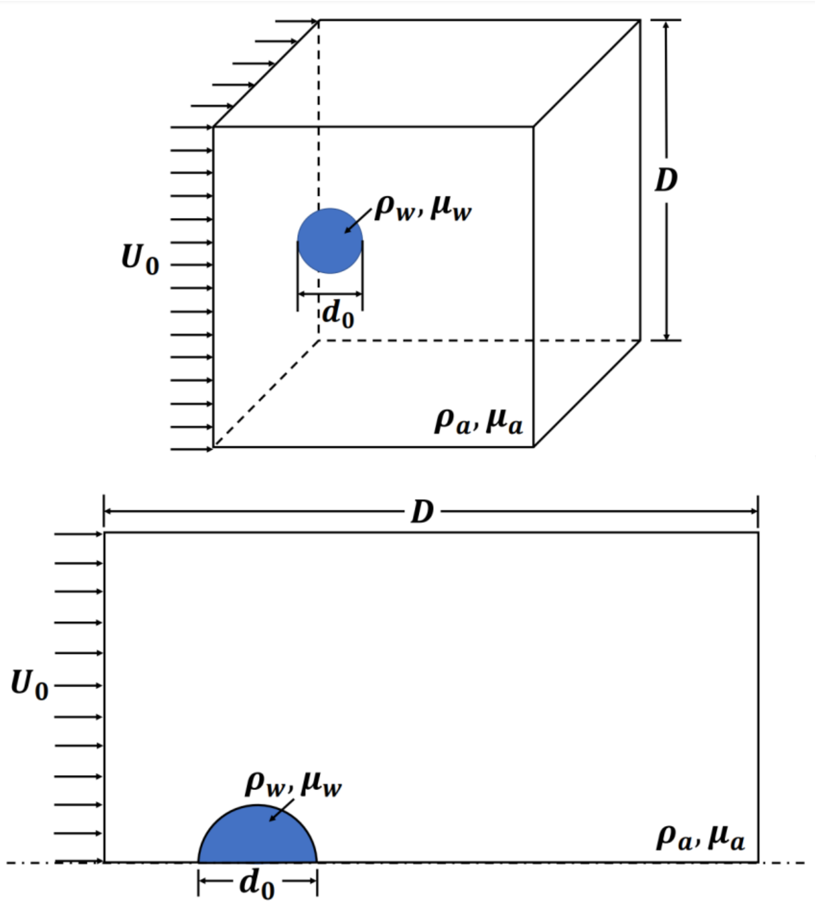

Fig. 5 Sketches showing initial configuration of flow fields in 3D (upper) and axisymmetrical (lower) simulations.

[1] Available at: http://basilisk.fr/

Numerical Setup

- VOF Breakup

  Film breaks when its thickness reaches $\Delta = \frac{D}{2^{L_{\mathbf{grid}}}}$ (set by AMR)

  NS Equation does not describe topological change mechanisms

  Film breakup is unphysical, numerically uncontrolled and grid-dependent

- Solution: Manifold Death (MD) Algorithm [1]

  Detects films with thickness around $h_c = \frac{3D}{2^{L_{\mathbf{sig}}}}$ with a period $T_{\mathbf{MD}}$

  Artificial film perforation with prescribed probability p

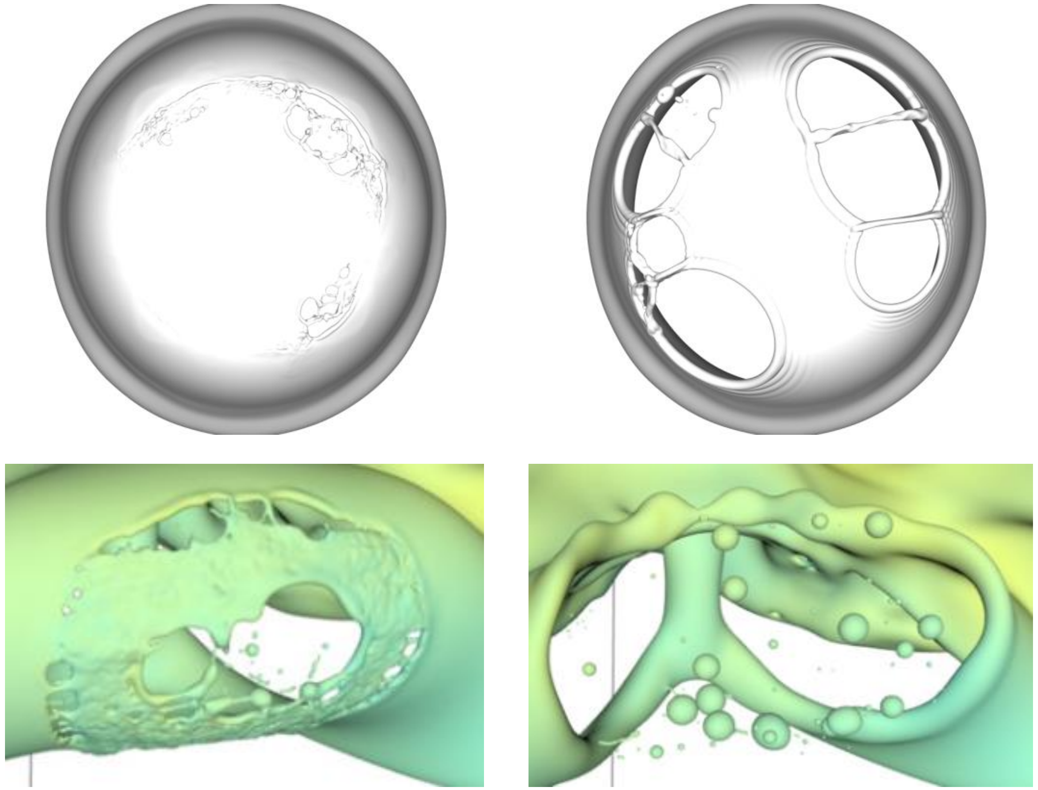

3D atomization simulations with default (uncontrolled) perforation and controlled perforation by the MD algorithm. Upper row: snapshots of present aerobreakup simulations at GridL = 12 and 13; Lower row: snapshots of the phase inversion test from [1].

[1] Chirco, L., Maarek, J., Popinet, S., & Zaleski, S. (2022). Manifold death: a Volume of Fluid implementation of controlled topological changes in thin sheets by the signature method. *Journal of Computational Physics*, 467, 111468.

Grid Convergence of Fragment Statistics

- Manifold Death (MD) algorithm parameters [1]

  $$p = \frac{1}{17500}, L_{\mathrm{sig}} = 13, T_{\mathrm{MD}} = 0.5$$

- Convergence of fragment statistics with $d \geq 8\Delta_{13}$ and fixed L_{sig}

  Agreement with log-normal fit for experimental results in [1]

- Fragments with $d < 8\Delta_{13}$ not reaching grid convergence

  Ligament breakup not controlled by MD

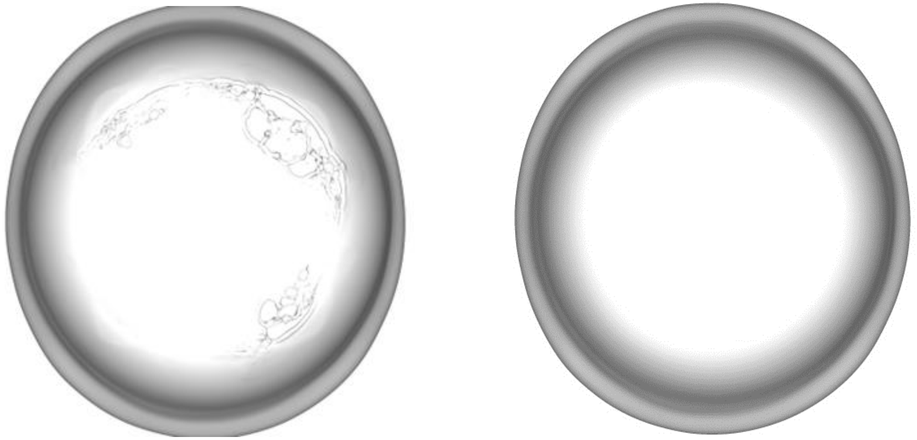

Droplet aerobreakup at GridL14, SigL13, with $We = 15, Oh = 0.001$.

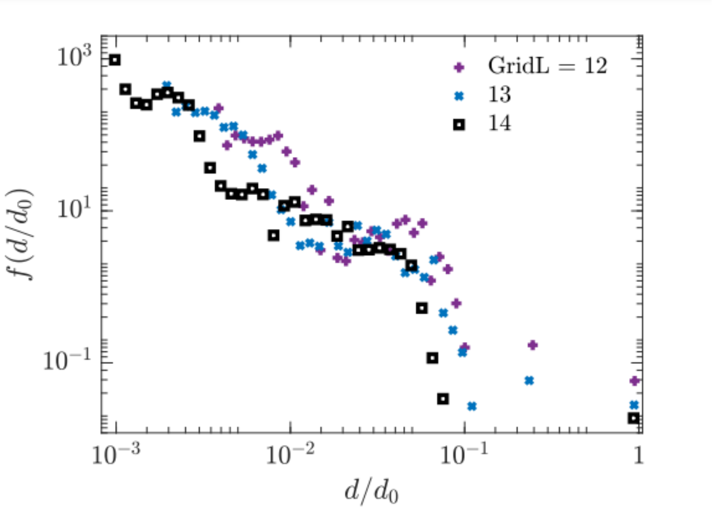

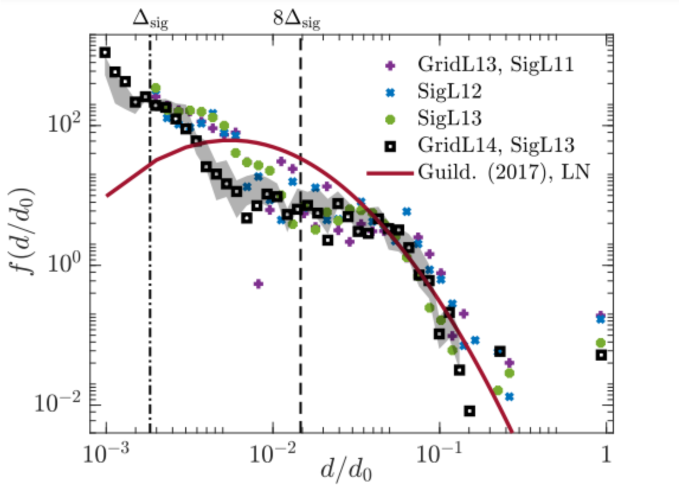

Grid convergence study showing the time- and ensemble-averaged size distribution of aerobreakup fragments without (left) and with (right) the MD algorithm applied. For all cases $We = 15, Oh = 0.001$.

[1] Chirco, L., Maarek, J., Popinet, S., & Zaleski, S. (2022). Manifold death: a Volume of Fluid implementation of controlled topological changes in thin sheets by the signature method. *Journal of Computational Physics*, 467, 111468.

[2] Guildenbecher, D. R., Gao, J., Chen, J., & Sojka, P. E. (2017). Characterization of drop aerodynamic fragmentation in the bag and sheet-thinning regimes by crossed-beam, two-view, digital in-line holography. *International Journal of Multiphase Flow*, 94, 107-122.

Breakup Phenomena: Ligament Breakup

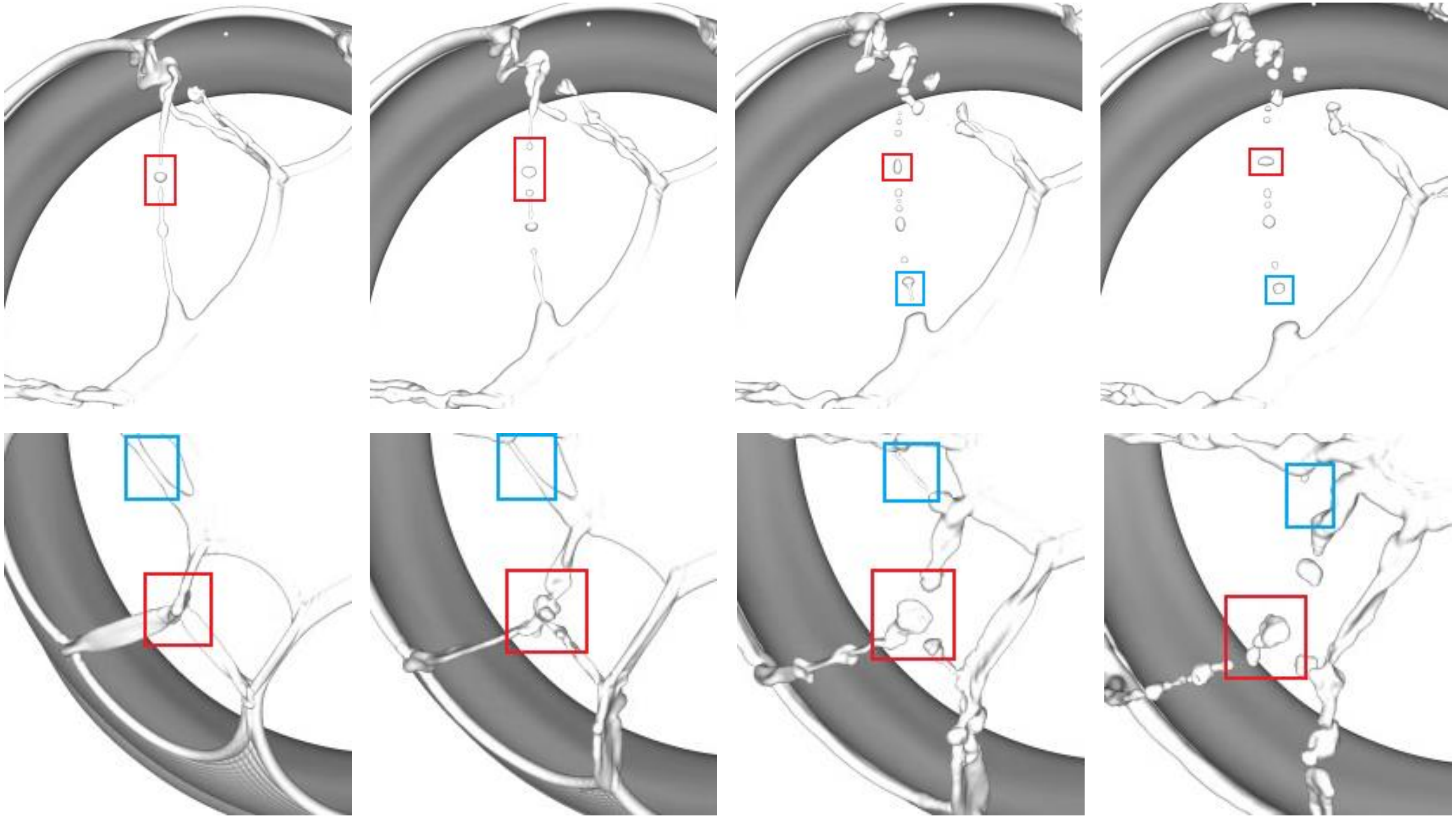

Breakup of a long ligament (upper row), a short ligament and a liquid node (lower row), with $We = 15, Oh = 0.001$.

- **Long ligament breakup**
  - Production of primary and satellite fragments with different sizes
  - Oblate-prolate oscillation of primary drops
  - Remerging of satellite drops with primary drops
- **Short ligament breakup**
  - Formation of a single drop
- **Large node detachment**
  - Successive breakup of bordering ligaments
  - Large-amplitude corrugation patterns – nonlinear oscillation

Breakup Phenomena: Rim Instability and Collision

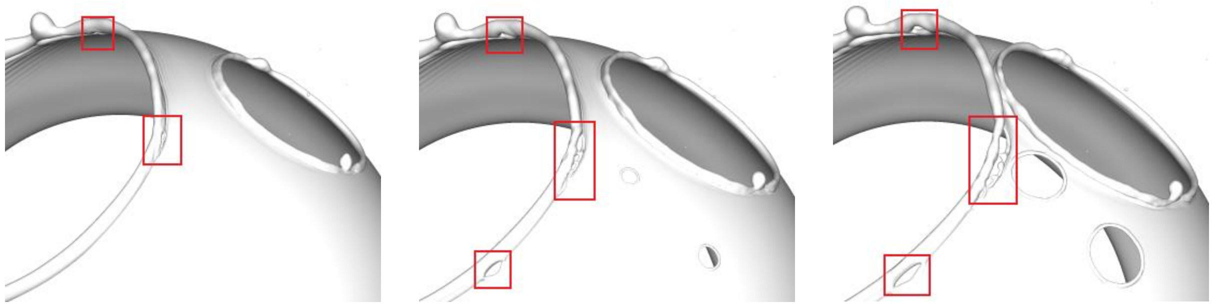

Destabilization of a receding rim on the bag surface with $We = 15$, $Oh = 0.001$, GridL = 14, SigL = 13.

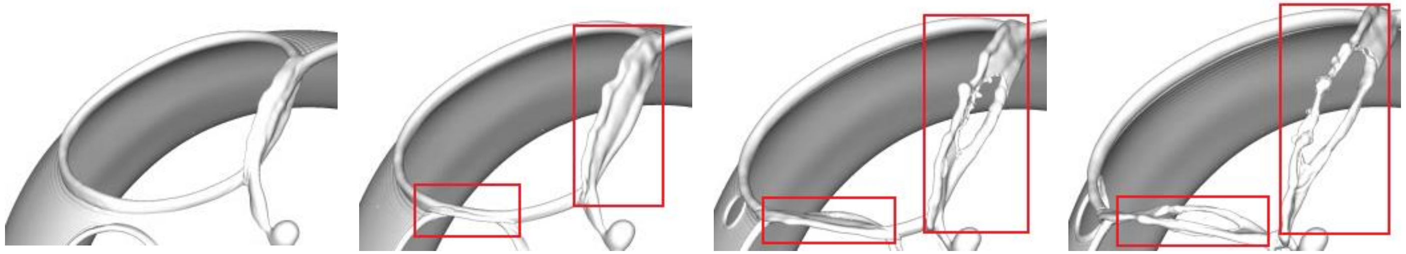

Evolution of 'fingering' liquid lamellae during bag film fragmentation with $We = 15$, $Oh = 0.001$, GridL = 14, SigL = 13.

- Destabilisation of receding rims
  - **Corrugation growth and film opening at rim foot**
  - Many hypotheses for the governing mechanism (RT, RP, etc. [1])
  - Complicated by drop acceleration, film thinning and non-uniform film curvature
- Rim collision
  - **Lamella formation in the transverse plane** [2]
  - Hole opening on the lamella
  - No ejection of fine drops

[1] Jackiw, I. M., & Ashgriz, N. (2022). Prediction of the droplet size distribution in aerodynamic droplet breakup. *Journal of Fluid Mechanics*, 940.
[2] Néel, B., Lhuissier, H., & Villermaux, E. (2020). 'Fines' from the collision of liquid rims. *Journal of Fluid Mechanics*, 893, A16.

Fragment Behaviour: Surface Oscillation

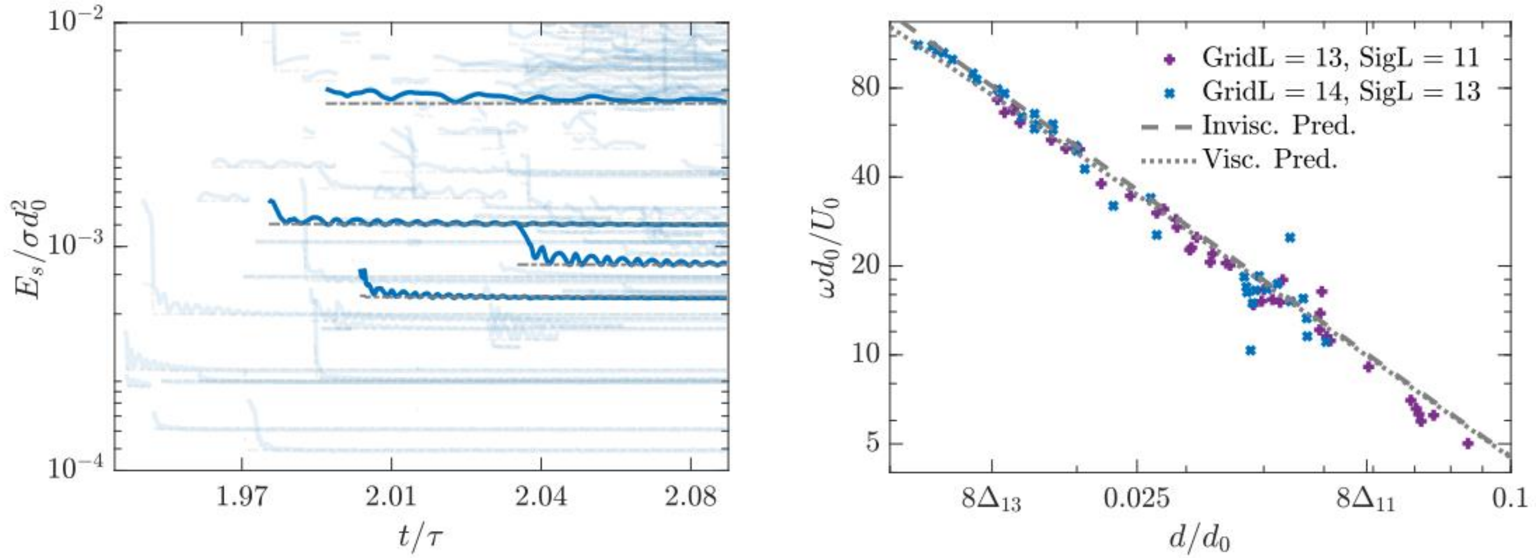

Left: evolution of fragment surface energy; right: frequency of the dominant mode of fragment oscillation as a function of fragment radius, with theoretical prediction of [2] superimposed

- Droplet tracking toolbox [1] for reconstructing breakup lineage and time evolution of individual fragments
- Regular oscillation patterns in fragment surface energy

  Smaller fragments oscillate quicker
- Good agreement with Prosperetti's theory [2]: $\omega_{n,0}^2 = (n-1)n(n+2)\dfrac{\sigma}{\rho_l R_0^3}$

  Fragment oscillation dominated by the 2nd Rayleigh mode ($n = 2$).
- Behaviour of small fragments well resolved

[1] Chan, W. H. R., Dodd, M. S., Johnson, P. L., & Moin, P. (2021). Identifying and tracking bubbles and drops in simulations: A toolbox for obtaining sizes, lineages, and breakup and coalescence statistics. *Journal of Computational Physics*, 432, 110156.
[2] Prosperetti, A. (1980). Free oscillations of drops and bubbles: the initial-value problem. *Journal of Fluid Mechanics*, 100(2), 333-347.

Laminar Bag Breakup

Tang, K., Adcock, T. A. A., & Mostert, W. (2023). Bag film breakup of droplets in uniform airflows. Journal of Fluid Mechanics, 970, A9. Featured on Cover.

Turbulent Bag Formation

Tang, K., Adcock, T. A. A., & Mostert, W. (2025). Droplet bag formation in turbulent airflows. Physical Review Fluids, 10(3), 033604. Selected as Editor’s Suggestion

Introduction: Turbulence Effects on Aerobreakup

- **Grid convergence for fragment statistics [1]**

  Agreement with experiments for large fragment sizes

- Bag fragmentation mechanisms:

  Hole expansion;

  Rim collision and destabilization;

  Ligament and node breakup.

- **Effects of air-phase turbulence**

  Characteristic of wind-wave boundary layers [2]

  Significant changes in aerobreakup phenomena [3]

  - Longer, wider and more distorted bags
  - Additional breakup mechanisms

  Lack of a consistent research framework

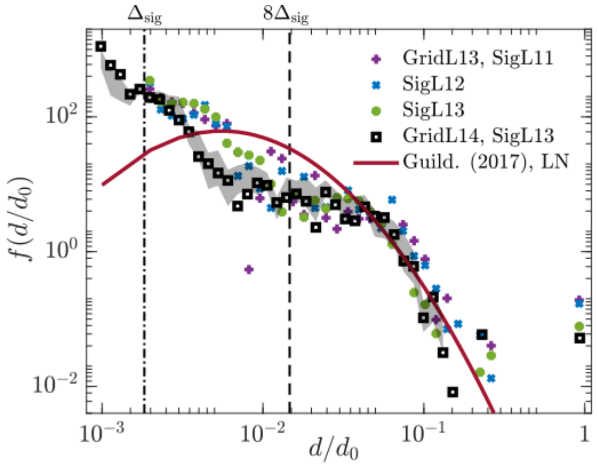

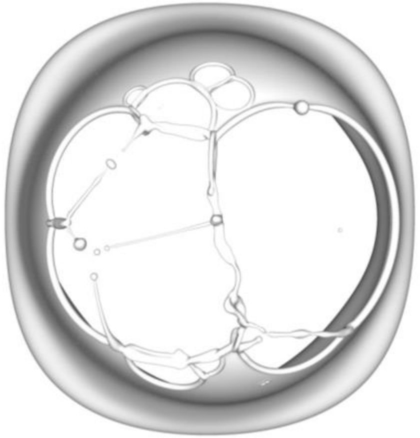

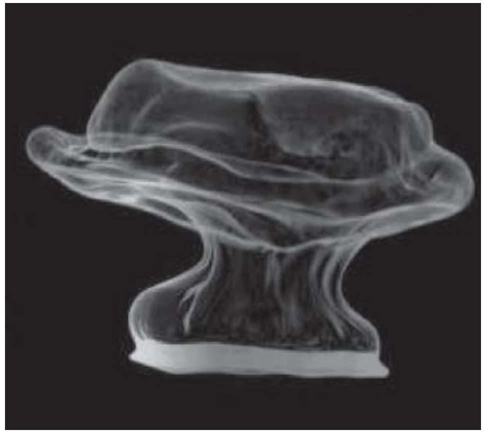

Morphology of breaking droplet and associated fragment size distributions in laminar and turbulent airflows [1][3]

[1] Tang, K., Adcock, T. A. A., & Mostert, W. (2023). Bag film breakup of droplets in uniform airflows. *Journal of Fluid Mechanics*, 970, A9.

[2] Wu, J., Popinet, S., & Deike, L. (2022). Revisiting wind wave growth with fully coupled direct numerical simulations. *Journal of Fluid Mechanics*, 951, A18.

[3] Zhao, H. et al. (2019). Effect of turbulence on drop breakup in counter air flow. *International Journal of Multiphase Flow*, 120, 103108.

Problem Configuration

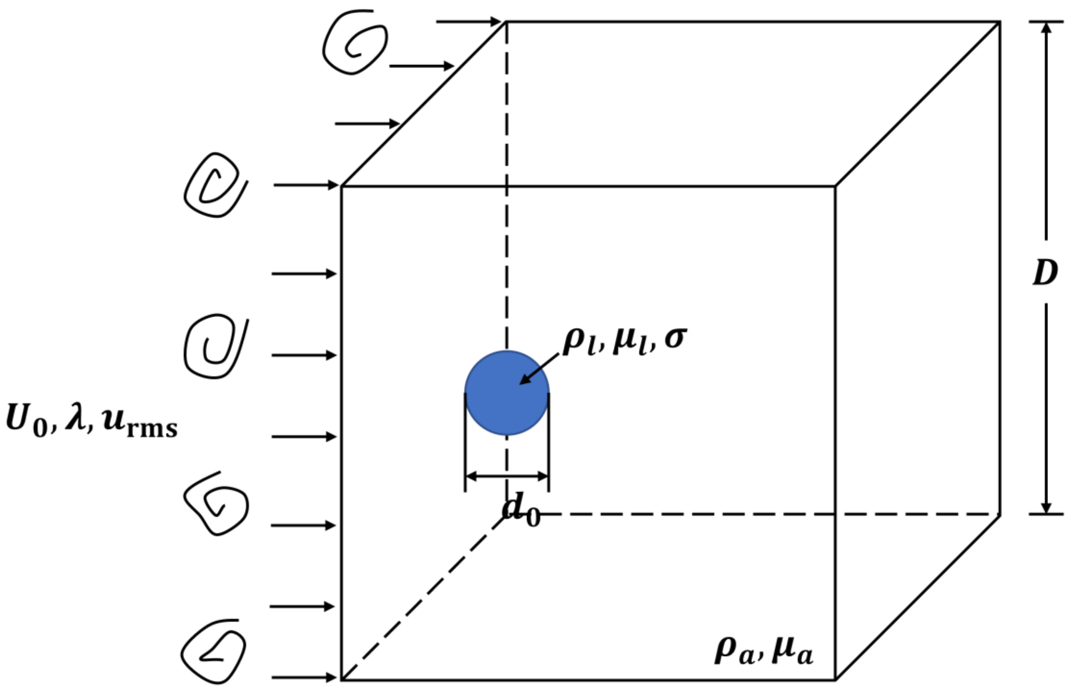

Schematic illustration showing the configuration for the turbulent aerobreakup problem.

- **Methodology**

Synthetic turbulence generation [1]

Impose pseudo-turbulence on a uniform base flow

Insert droplet after airflow becomes statistically stationery

Basilisk, Two-Phase NS Equation w. AMR [2]

- **Non-Dimensional Parameters**

$$\rho^* \equiv \frac{\rho_l}{\rho_g} = 833, \qquad \mu^* = \frac{\mu_l}{\mu_g} = 55,$$

$$We \equiv \frac{\rho_g U_0^2 d_0}{\sigma}, \qquad Oh \equiv \frac{\mu_l}{\sqrt{\rho_l \sigma d_0}}, \qquad \frac{\boldsymbol{u_{rms}}}{\boldsymbol{U_0}}, \qquad \frac{\boldsymbol{L_{La}}}{\boldsymbol{R_0}}$$

[1] Xie, Z. T., & Castro, I. P. (2008). Efficient generation of inflow conditions for large-eddy simulation of street-scale flows. *Flow Turbulence and Combustion*, 81(3), 449-470.
[2] S. Popinet (2019), Basilisk flow solver and PDE library, available at: http://basilisk.fr

Overview of Bag Morphology

$(u_{rms}/U_0, L_{La}/R_0) = (0.25, 1)$ $(0.5, 1)$ $(0.65, 1)$ $(0.8, 1)$

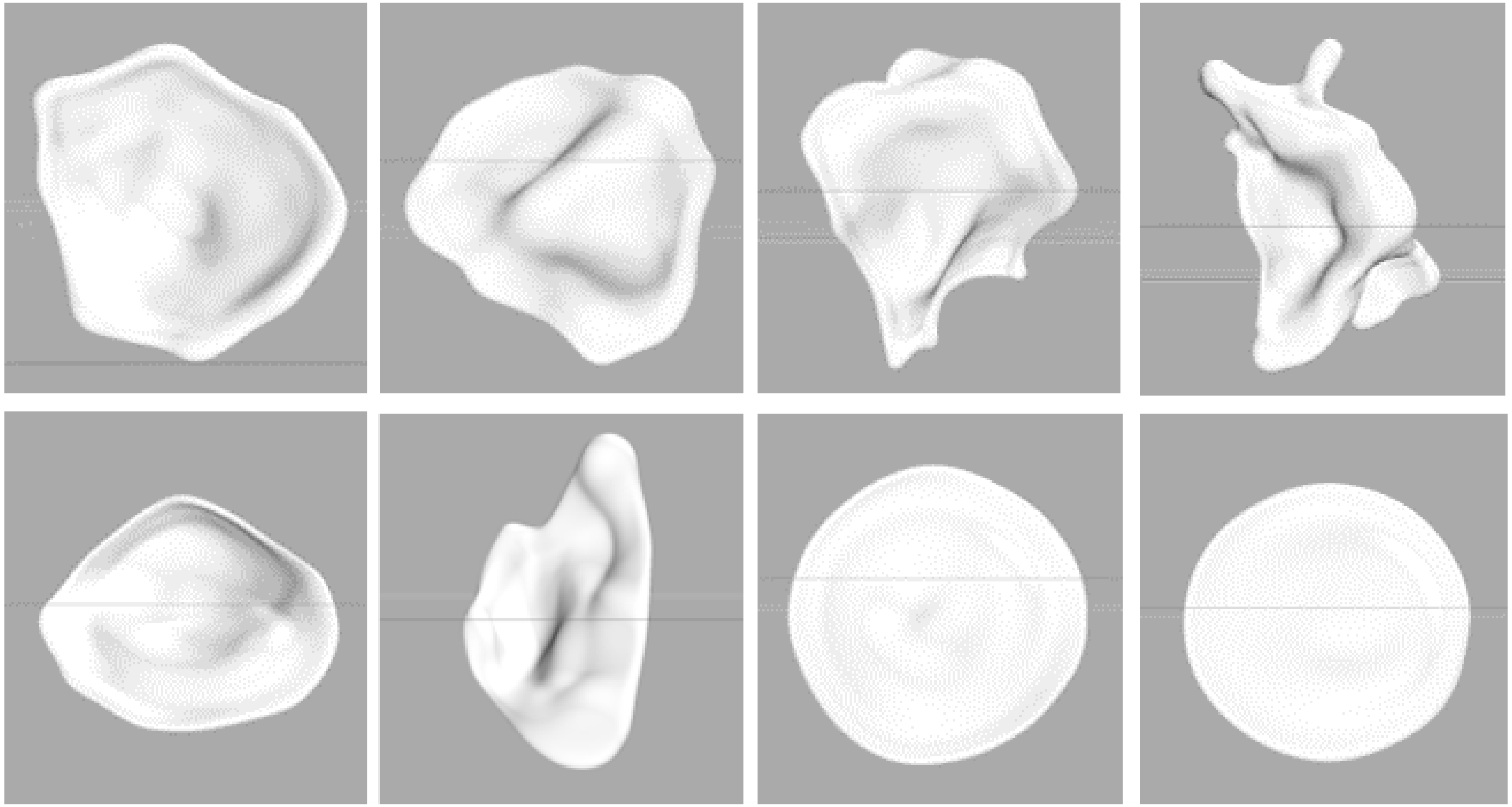

$(0.25, 1.5)$ $(0.25, 2)$ $(0.25, 4)$ $(0.25, 8)$

Increasing u_{rms} / decreasing L_{La}:

More corrugations

Peripheral nodes

Global distortion

Distinction between rim and bag less prominent

Decreasing u_{rms} / increasing L_{La}:

Recovery of laminar bag shape

Global Deformation Characteristics

Spherical harmonic decomposition:
 Mode-2 deformation dominates droplet flattening
Bag lengths and widths not defined:
 Aspect ratio $\sqrt{I_1/I_3}$ (eigenvalues of the moment-of-inertia tensor)

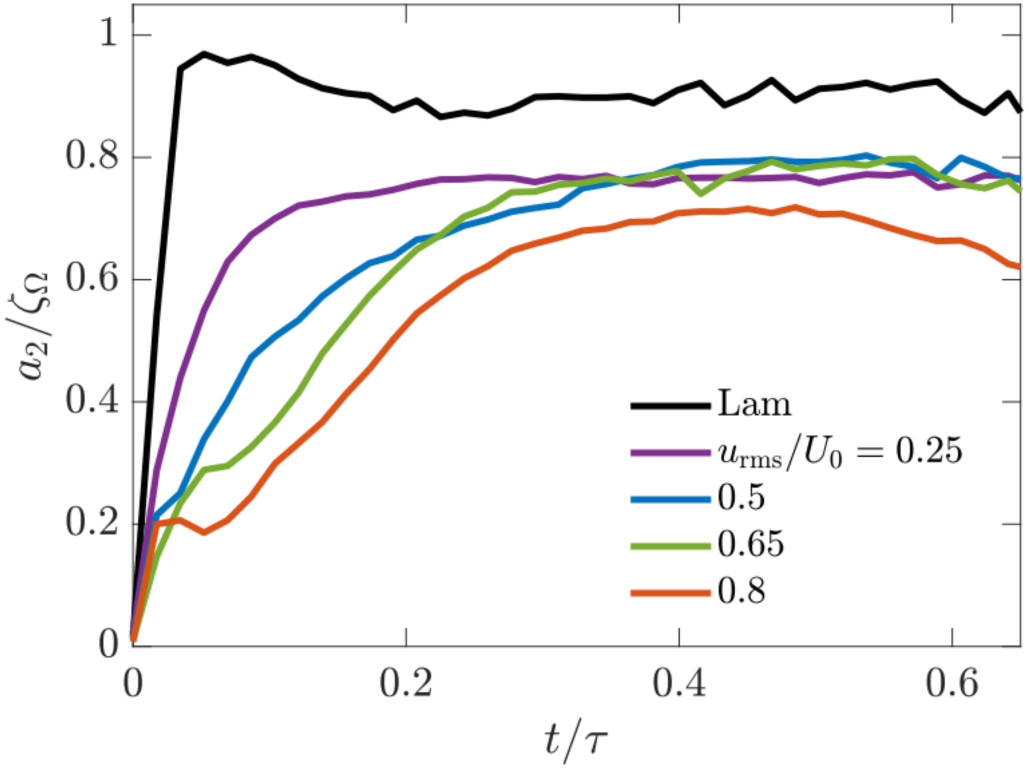

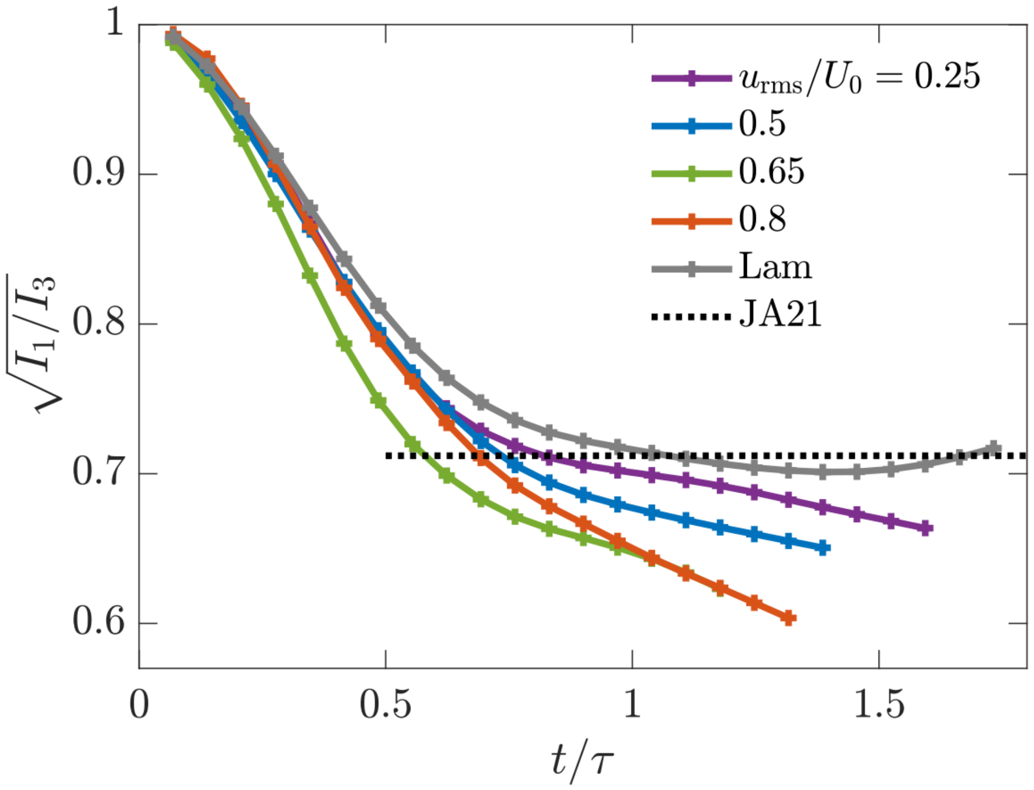

Evolution of mode-2 deformation a_2 (left) and droplet aspect ratio $\sqrt{I_1/I_3}$ (right)

[1] Jackiw, I. M., & Ashgriz, N. (2021). *On aerodynamic droplet breakup*. Journal of Fluid Mechanics, 913, A33.

Droplet Tilting Dynamics

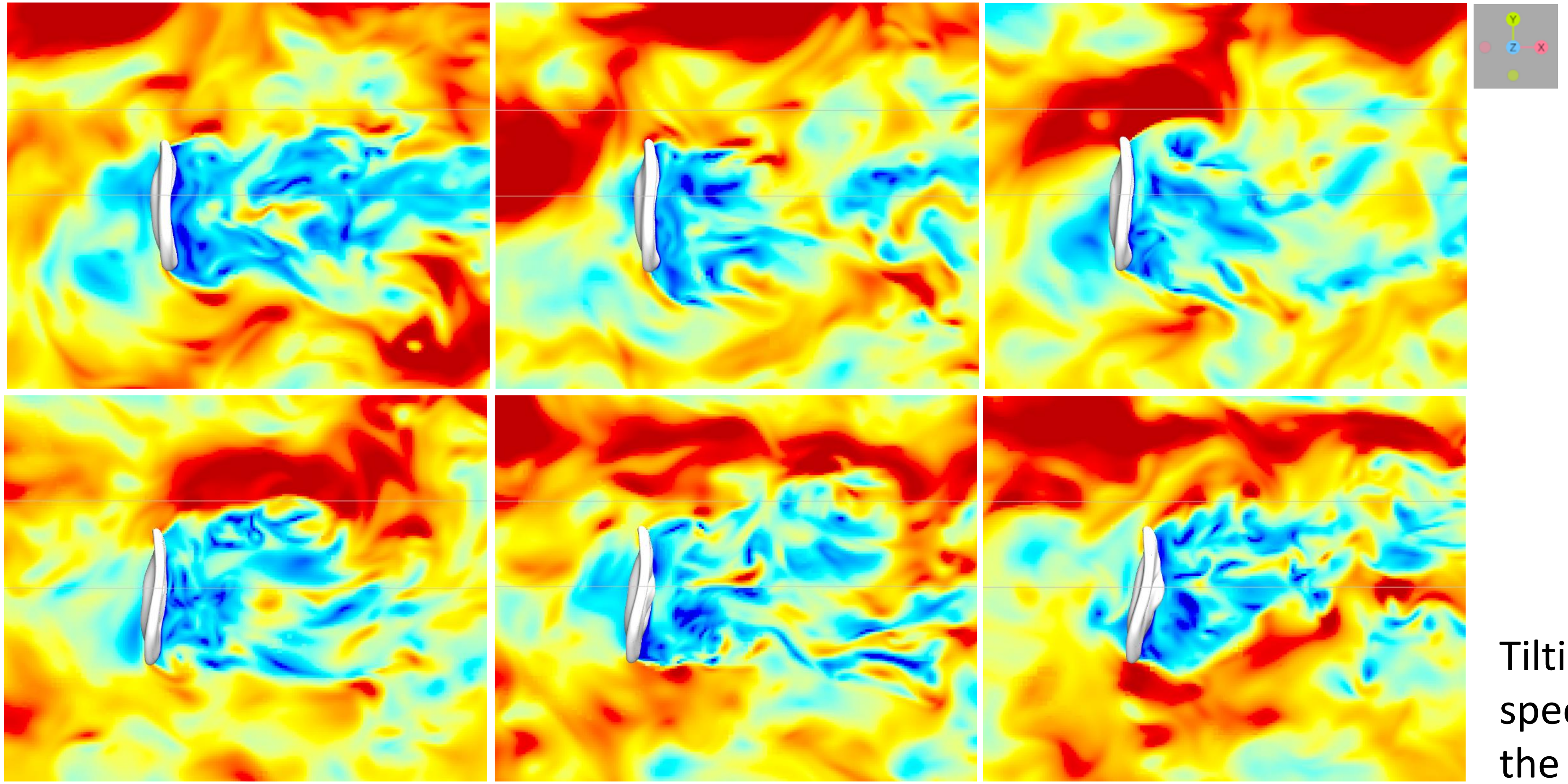

Simulation snapshots taken for $u_{rms} = 0.25U_0, L_{La} = 2R_0, t/\tau_0 = 1.03 - 1.32$. The flow field is coloured based on the local airflow speed.

Tilting triggered by high-speed air parcels bypassing the flattened droplet

Droplet Tilting Dynamics

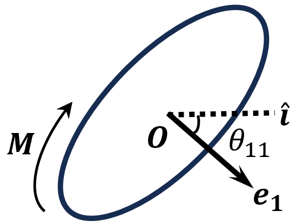

Droplet orientation angle:
$\theta_{11} = \arccos(\boldsymbol{e_1} \cdot \hat{\boldsymbol{i}})$;
Hydrodynamic torque : $\boldsymbol{M} = \iint \boldsymbol{r} \times \left(-p\delta_{mn} + 2\mu_g S_{mn}\right) d\boldsymbol{S}$

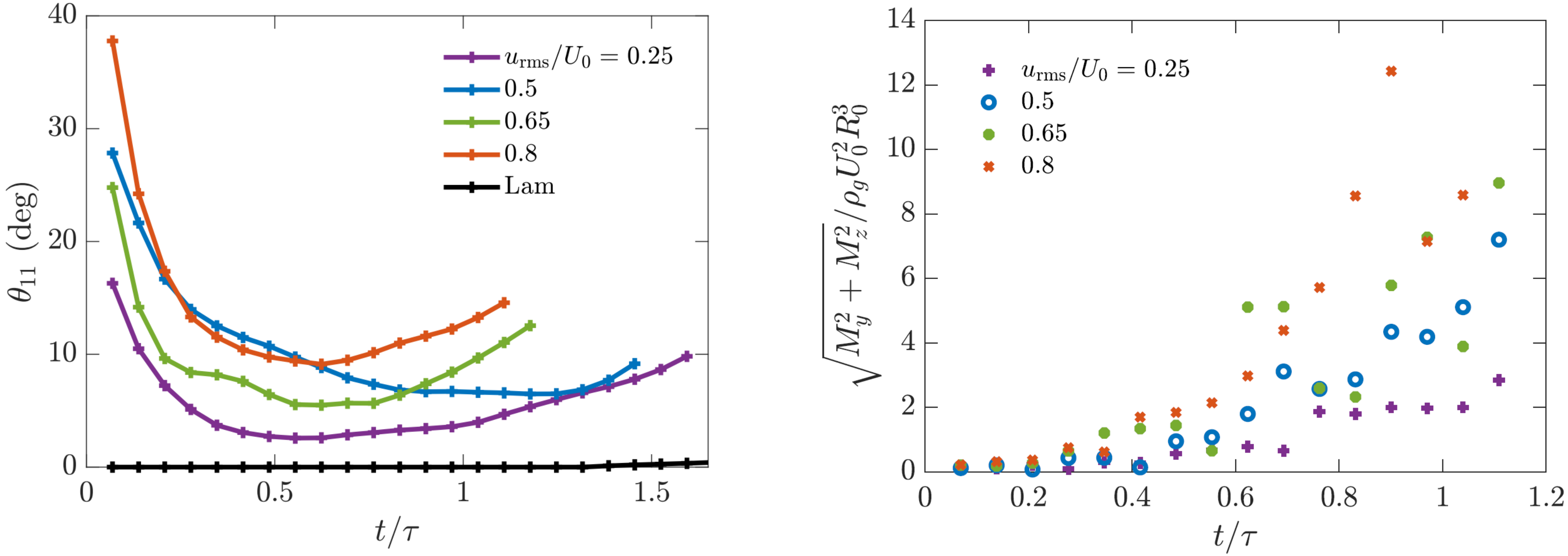

Evolution of the droplet orientation angle θ_{11} (left) and hydrodynamic torque M_{yz} (right).

Rapid torque growth causes droplet tilting

Distribution of local surface curvature

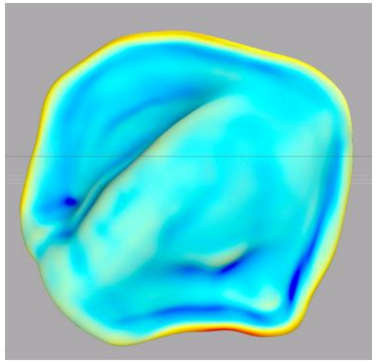

Impact of turbulent eddies on flattened bag surfaces

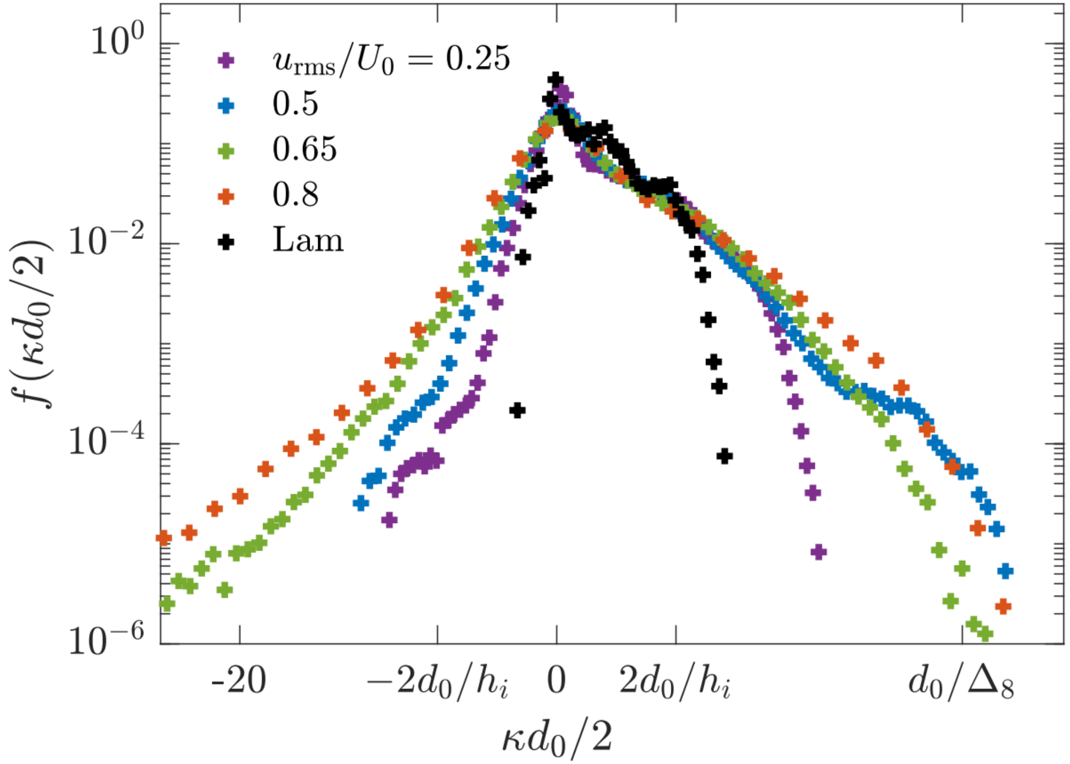

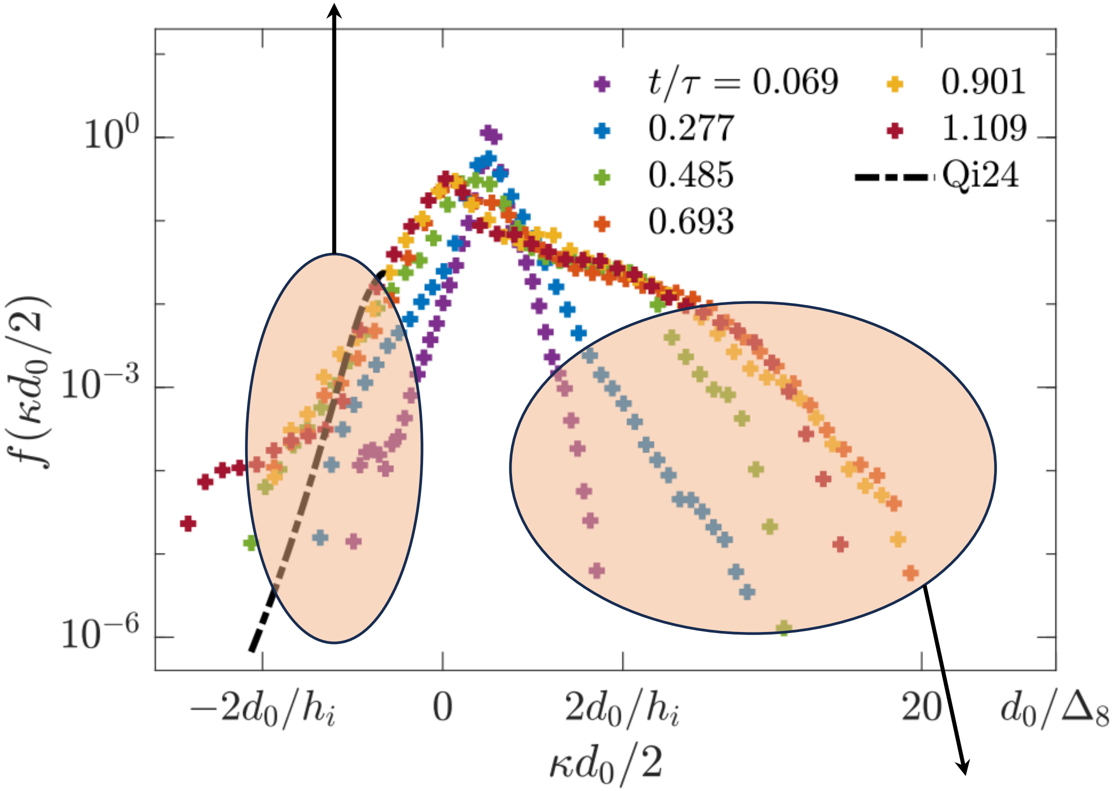

Formation of peripheral rims and nodes

Broadening of the distribution of curvature κ most prominent at the right tail.

[1] Qi, Y., *et al*. (2024). Breaking bubbles across multiple time scales in turbulence. *Journal of Fluid Mechanics*, 983, A24.

Conclusions and Future Work

- Laminar and turbulent aerobreakup simulations;
- Used MD algorithm to control film perforation;
- Establishment of grid convergence for large fragment statistics;
- Late-time bag film fragmentation:

  Rim collision and destabilization

  Ligament and node breakup

  Fragment oscillation patterns
- Turbulent aerobreakup

  Characterisation of surface deformation patterns

  Quantification of droplet tilting behaviour

  Broadening of surface curvature distributions

Conclusions and Future Work

- ☐ Fully resolved film perforation at higher grid resolution levels
- ☐ Bag breakup in turbulent airflows
  - ☐ Development of physically informed Sea Spray Generation Functions
- ☐ Effects of surfactants, evaporation, etc.
  - ☐ Accounting for spume generation with realistic sea states

Thanks for your attention!

Acknowledgments

- EPSRC for accessing the UK supercomputing facility ARCHER2 via the UK Turbulence Consortium (EP/R029326/1)
- Oxford Advanced Research Computing (ARC) facility

- Tang, K., Adcock, T. A. A., & Mostert, W. (2023). *Bag film breakup of droplets in uniform airflows*. Journal of Fluid Mechanics, 970, A9. Featured on Cover.
- Tang, K., Adcock, T. A. A., & Mostert, W. (2025). *Droplet bag formation in turbulent airflows*. Physical Review Fluids, 10(3), 033604. Selected as Editor’s Suggestion.